

TOVAC: Tele-operated Vehicle Admission Control and Routing

Jorge Martín-Pérez, Carlos M. Lentisco, Luis Bellido, Ignacio Soto, and David Fernández

Abstract—Tele-operated Driving (ToD) is a challenging use case for mobile network operators. Video captured by the built-in vehicle cameras must be streamed meeting a latency requirement of 5 ms with a 99.999% reliability. Although 5G offers high bandwidth, ultra-low latencies and high reliability; ToD service requirements are violated due to bad channel conditions. Ignoring the channel state may lead to over-estimate the number of ToD vehicles that can meet the service requirements, hence comprising the vehicle security. To fill this gap, in this letter we propose TOVAC, an algorithm that guarantees ToD service requirements by taking adequate admission control and routing decisions. This is achieved by using a channel-based capacity graph that determines the maximum number of vehicles that can be tele-operated in any road section. We evaluate TOVAC considering cellular deployments from Turin and show that, unlike a state of the art solution, TOVAC guarantees the ToD service requirements.

Index Terms—Tele-operated Driving, quality assurance, reliability, traffic control, routing.

I. INTRODUCTION

The aim of ToD vehicles is to allow drivers to operate vehicles from safer and more comfortable locations, or to provide remote operator assistance in situations where an automated driving system is facing ambiguous situations. Remotely operated vehicles send their status and environment information (e.g., gathered with cameras, LIDAR and other sensors) to the remote operator through a wireless network channel. This information is presented to the operator, which sends back control or assistance commands to the vehicle through the network [1].

The exchange of information between the remote operations centre and the tele-operated vehicles requires a network service that meets the Quality of Service (QoS) requirements defined in [2]. QoS degradation can pose a significant threat to road safety, which translates into the need to adapt the vehicular application profile to QoS variations, for example, by decreasing the video streaming bitrate [3] and reducing vehicle speed or even making an emergency stop.

5GAA has explored how a remote driver should be warned in these situations to adapt ToD to the existing level of QoS [4]. However, the standards are yet far from preventing

This work was supported by the Remote Driver project (TSI-065100-2022-003) funded by Spanish Ministry of Economic Affairs and Digital Transformation, and the ECTICS project (PID2019-105257RB-C21), funded by the Spanish Ministry of Economy and Competitiveness, and the Spanish Ministry of Science and Innovation.

The authors are with ETSI Telecomunicación, Universidad Politécnica de Madrid, Spain, e-mail: jorge.martin.perez@upm.es.

©2023 IEEE. Personal use of this material is permitted. Permission from IEEE must be obtained for all other uses, in any current or future media, including reprinting/republishing this material for advertising or promotional purposes, creating new or redistribution to servers or lists, or reuse of any copyrighted component of this work in other work

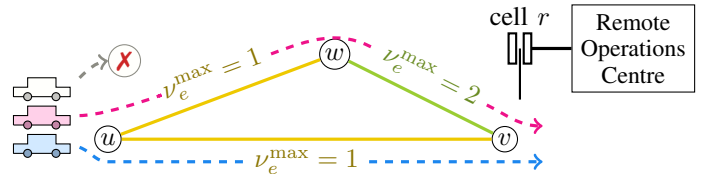


Fig. 1. Illustration of the edges within TOVAC capacity graph, each with the maximum number of ToD vehicles admitted ν_e^{\max} . Further roads have smaller capacity (yellow) due to path loss, while a road nearby the cell r (green) has higher capacity. Consequently, TOVAC just admits the first two vehicles and rejects the third (top vehicle), since cell r only guarantees the ToD service requirements for a single vehicle $\nu_e^{\max} = 1$ at roads (u, w) , (u, v) .

the QoS degradation. Although the Third Generation Partnership Project (3GPP) Network Slice Admission Control Function (NSACF) [5] limits the admission per network slice, it does not prevent too many terminals from registering simultaneously to the same cell. Thus, the NSACF cannot prevent QoS degradation due to congestion.

To avoid video quality degradations, Liu *et al.* [6] propose a *static* routing and traffic control framework that decides: the vehicle routes, the maximum distance between vehicles, their speed, and the bandwidth allocated at each cell to the remote driving service. That is, authors propose adjusting the video bitrate of each vehicle to the available bandwidth at each cell, neglecting the experienced latency and reliability.

However, the QoS of a ToD service can also be affected by latency and reliability, as discussed by Liu *et al.* in [6, §III, §VI]. Motivated by such statement, this letter describes Tele-operated Vehicle Admission Control and Routing (TOVAC), an admission control and routing algorithm that also meets the latency and reliability requirements defined by the 3GPP for ToD [2, Table 5.5-1]: (i) a Packet Delay Budget (PDB) shorter than 5 ms; and (ii) a 99.999% reliability. Additionally, TOVAC (iii) does not impose a speed reduction of vehicles; and (iv) solves the admission control problem avoiding overlaps in time.

TOVAC calculates the channel capacity using the 99.999-percentile of the Signal to Interference plus Noise Ratio (SINR) to determine the maximum number of vehicles that can be tele-operated along the roads while meeting the 5 ms PDB requirement. Specifically, TOVAC creates a capacity graph such as the one illustrated in Fig. 1, with each edge e representing a road with an associated capacity of ν_e^{\max} tele-operated vehicles. TOVAC receives, concurrently, several requests to obtain their routes (three in Fig. 1), finding the shortest path for each vehicle without incurring into QoS violations. As Fig. 1 shows, TOVAC admits the first two vehicles but rejects the third (the white vehicle at the top) because the serving cell r does not have enough capacity ν_e^{\max} to meet the QoS requirements at roads (u, w) and (u, v) .

II. NEW RADIO (NR) TOD CAPACITY MODEL

In this section we describe a model to obtain the maximum number of ToD vehicles at each road segment. First, we obtain the radio resources needed to meet the service PDB at a road segment. Then, we compute the 99.999% spectral efficiency

for a vehicle at a specific coordinate served by a cell. Lastly, we use the two previous results to create a road capacity graph whose weights are the maximum number of vehicles that have enough radio resources to meet the PDB with 99.999% probability.

A. Radio resources for remote driving

At the radio resources level, our approach is to guarantee the availability of enough Resource Block (RB)s to send the ToD service packets within the timespan of a PDB. Assuming a packet size of L bits, each packet consumes:

$$R(S_r^\nu, \mu, L) = \left\lceil \frac{L}{T_S^\mu 12\Delta f^\mu S_r^\nu} \right\rceil [\text{RB}/\text{packet}] \quad (1)$$

with $T_S^\mu = \frac{10^{-3}}{14 \cdot 2^\mu}$ [sec] symbol duration with numerology μ , $12 \cdot \Delta f^\mu$ [Hz/RB] the bandwidth of an RB using 12 subcarriers in the frequency domain, and S_r^ν the Spectral Efficiency (SE) [bps/Hz] for a vehicle ν that is served by cell r .

Considering a maximum service bitrate of b [bps] during any timespan of t [sec], each vehicle ν will send $\lceil \frac{b \cdot t}{L} \rceil$ packets of size L . Hence, in t sec each vehicle ν generates:

$$\alpha_\nu(t, S_r^\nu, \mu, b, L) = R(S_r^\nu, \mu, L) \left\lceil \frac{b \cdot t}{L} \right\rceil [\text{RB}] \quad (2)$$

For a set of vehicles N_r requesting service from cell r we can select the maximum number of RB generated by any vehicle to obtain the maximum number of vehicles that can be served meeting a PDB of D :

$$\nu_r^{\max}(D, \mu, b, L) = \left\lfloor \frac{\lfloor (1 - OH) \cdot \text{NRB}_r(D, B) \rfloor}{\max_{\nu \in N_r} \alpha_\nu(D, S_r^\nu, \mu, b, L)} \right\rfloor [\text{veh}] \quad (3)$$

In (3) OH is the signaling overhead in NR and $\text{NRB}_r(D, B)$ the number of RBs available for the ToD service in D [sec] at a cell r using a bandwidth of B [MHz].

B. Cell Spectral Efficiency

With (3) we obtain a worst-case value for the number of vehicles that can be served by a cell. But note that the number of RBs that each vehicle needs depend on the SE (1), with lower SE leading to a larger number of required RBs.

To obtain SE we first need to compute the SINR. Specifically, we obtain the SINR Complementary Cumulative Distribution Function (CCDF) to know, e.g., whether a vehicle experiences a SINR $\gamma_{r,\nu} = 20$ dB with 99.999% probability. We resort to a probabilistic model as the proposed in [7], [8] to obtain the following expression.

Corollary 1. *If the cell power follows an exponential distribution $h \sim \exp(\mu)$, and the interfering cells power is also exponential and identically distributed $g_i \stackrel{i.i.d}{\sim} \exp(\lambda)$; the SINR CCDF satisfies*

$$\mathbb{P}[\gamma_{r,\nu} > \hat{\gamma}] = e^{-\mu \hat{\gamma} d_{r,\nu}^\alpha \sigma^2} \prod_i \frac{\lambda}{\lambda + \mu \hat{\gamma} d_{r,\nu}^\alpha d_{r_i,\nu}^{-\alpha}} \quad (4)$$

with $\alpha > 0$ the path loss exponent, σ^2 the value of additive and constant noise power, and $d_{r,\nu}$ the distance between cell r and vehicle ν .

Proof. The SINR is expressed as $\gamma = h d_{r,\nu}^{-\alpha} (\sigma^2 + I_r)^{-1}$ with $h d_{r,\nu}^{-\alpha}$ the received power, $h \sim \exp(\mu)$, and $I_r = \sum_i g_i d_{r_i,\nu}^{-\alpha}$ being the neighboring interference experienced by the vehicle ν assuming $g_i \stackrel{i.i.d}{\sim} \exp(\lambda)$. Hence

$$\begin{aligned} \mathbb{P}(\gamma > \hat{\gamma}) &= \mathbb{P}(h > \hat{\gamma} d_{r,\nu}^\alpha (\sigma^2 + I_r)) \\ &= \mathbb{E}_{I_r} [\mathbb{P}(h > \hat{\gamma} d_{r,\nu}^\alpha (\sigma^2 + I_r) | I_r)] = \mathbb{E}_{I_r} \left[e^{-\mu \hat{\gamma} d_{r,\nu}^\alpha (\sigma^2 + I_r)} \right] \\ &= e^{-\mu \hat{\gamma} d_{r,\nu}^\alpha \sigma^2} \cdot \mathcal{L}_{I_r}(\mu \hat{\gamma} d_{r,\nu}^\alpha) \quad (5) \end{aligned}$$

with $\mathcal{L}_{I_r}(s)$ the Laplace transform of the neighboring interference, which has the following expression

$$\begin{aligned} \mathcal{L}_{I_r}(s) &= \mathbb{E}_{I_r} [e^{-s I_r}] = \mathbb{E}_{\{g_i\}} \left[e^{-s \sum_i g_i d_{r_i,\nu}^{-\alpha}} \right] \\ &= \mathbb{E}_{\{g_i\}} \left[\prod_i e^{-s g_i d_{r_i,\nu}^{-\alpha}} \right] = \prod_i \mathbb{E}_{g_i} \left[e^{-s g_i d_{r_i,\nu}^{-\alpha}} \right] \\ &= \prod_i \int_0^\infty e^{-s g d_{r_i,\nu}^{-\alpha}} \lambda e^{-\lambda g} dg = \prod_i \frac{\lambda}{\lambda + s \cdot d_{r_i,\nu}^{-\alpha}} \quad (6) \end{aligned}$$

By plugging (6) into (5), (4) holds. \square

Using Corollary 1 we compute the 99.999% SINR as $\hat{\gamma} : \mathbb{P}(\gamma \geq \hat{\gamma}) \geq 0.99999$. To compute the 99.999 percentile SE $S_r(\hat{\gamma})$ we use the Shannon capacity expression.

Given the 99.999 percentile SE, we just have to check which NR Modulation Coding Scheme (MCS) provides the closest SE. Specifically, we obtain the 99.999 percentile effective SE as:

$$\hat{S}_r(\hat{\gamma}) = \arg \min_{s \in S: S_r(\hat{\gamma}) > s} \{S_r(\hat{\gamma}) - s\} \quad (7)$$

with s the SE achieved by each MCS reported in [9, Table 6.1.4.1].

C. Road capacity graph

With Sections II-A and II-B we now calculate the maximum number of ToD vehicles that can be operated at each road. Specifically, we are interested in obtaining a weighted graph G with the roads as edges $e \in E(G)$ and the the maximum number of vehicles that can be operated at each road ν_e^{\max} as weights.

We define $E(r) \subset E(G)$ as the set of roads covered by cell r . For each road e served by cell r we select the worst effective SE:

$$\hat{S}_{r,e}(\hat{\gamma}) = \min_{x \in e} \hat{S}_r(\hat{\gamma}_x) \quad (8)$$

with $\hat{\gamma}_x$ the 99.999 percentile SINR provided by cell r at coordinate x within road e .

Using the the worst effective SE calculated with (8) we can re-formulate (3) to obtain the maximum number of vehicles served by cell r at road e :

$$\nu_{r,e}^{\max}(D, \mu, b, L) = \left\lfloor \frac{\lfloor \iota_r(e) \cdot (1 - OH) \cdot \text{NRB}_r(D, B) \rfloor}{\alpha_\nu(D, \hat{S}_{r,e}(\hat{\gamma}), \mu, b, L)} \right\rfloor \quad (9)$$

with $\iota_r(e) \in [0, 1]$ being the portion of RBs that cell r gives to road e .

Hence, the total maximum number of vehicles that can be operated at each road is

$$\nu_e^{\max}(D, \mu, b, L) = \sum_{r:e \in E(r)} \nu_{r,e}^{\max}(D, \mu, b, L) \quad (10)$$

The purpose of the capacity graph G is to use it for the admission control and routing of ToD vehicles. All we have to ensure is that there are no more than ν_e^{\max} vehicles at each road e .

III. TOD ADMISSION CONTROL AND ROUTING

In the previous section, the maximum number of ToD vehicles that can be operated on each road section has been determined. But there is still a need for a mechanism to control the path that vehicles follow along the road, so that the ToD service is denied if a vehicle attempts to enter a road section that has reached its maximum capacity.

We model this problem as a multi-commodity flow problem over time [10] on the capacity graph G defined in Section II-C.

Problem 1 (ToD Admission Control and Routing). *Given a fleet of ToD vehicles with their sources $\{s_\nu\}_\nu \subset G$ and destinations $\{d_\nu\}_\nu \subset G$, solve:*

$$\max_{X_{\mathcal{P}_\nu}^\nu} \sum_{\nu, \mathcal{P}_\nu} X_{\mathcal{P}_\nu}^\nu \quad (11)$$

$$s.t. : \sum_{\nu, \mathcal{P}_\nu} X_{\mathcal{P}_\nu}^\nu(e, t) \leq \nu_e^{\max}(D, \mu, b, L), \quad \forall t > 0, e \in G \quad (12)$$

with $X_{\mathcal{P}_\nu}^\nu(e, t) \in \{0, 1\}$ an auxiliary variable taking 1 if $e \in \mathcal{P} \wedge t \in [\tau_\nu(e^+), \tau_\nu(e^-)]$; and \mathcal{P}_ν a path with origin $s_\nu \in G$ and destination $d_\nu \in G$.

By solving the Problem 1, the number of vehicles flowing from their sources $\{s_\nu\}_\nu$ to their destinations $\{d_\nu\}_\nu$ is maximized. Constraint (12) ensures that no section of the road (e) carries more vehicles than those set by the capacity graph $\nu_e^{\max}(D, \mu, b, L)$. Therefore, constraint (12) ensures the ToD latency and reliability requirements.

In the formulation of the problem, each path is denoted as \mathcal{P} . The binary decision variable $X_{\mathcal{P}_\nu}^\nu(e, t)$ takes the value one if the vehicle ν is traversing the road section e at instant t , where e belongs to the path \mathcal{P} followed by the vehicle. The travel time of a vehicle in a road section is calculated as $\tau(e) = \tau_\nu(e^-) - \tau_\nu(e^+)$, being $\tau_\nu(e^+)$ and $\tau_\nu(e^-)$ the times at which the vehicle enters/exits road e . Hence, $\tau_\nu(e^+), \tau_\nu(e^-)$ are computed as follows:

$$\tau_\nu(e^+) = \sum_{\mathcal{P}} \sum_{e' \in \mathcal{P}: e' \prec e} X_{\mathcal{P}_\nu}^\nu \tau(e') \quad (13)$$

$$\tau_\nu(e^-) = \tau_\nu(e^+) + \tau(e) \quad (14)$$

with $e' \prec e$ denoting that road e' precedes road e in path \mathcal{P} .

Therefore, the total travel time of a vehicle, denoted as $\tau_\nu(\mathcal{P})$, can be calculated as the sum of the travel times on the road sections belonging to the path, i.e., as $\tau_\nu(\mathcal{P}) = \sum_{e \in \mathcal{P}} \tau(e)$.

To solve Problem 1 we propose Algorithm 1 (TOVAC), a modified version of the A^* search algorithm. The A^* algorithm

Algorithm 1 ToD Admission Control and Routing (TOVAC)

Require: $\{\nu_i\}_i, \{s_\nu\}_\nu, \{d_\nu\}_\nu, G$

- 1: $E(G) \setminus = \{e : \nu_e^{\max}(D, \mu, b, L) < 1\}$ \triangleright Prune roads
- 2: **for** $\nu \in \{\nu_i\}_i$ **do**
- 3: $\mathcal{P} = A^*(G, s_\nu, d_\nu, \text{weight} = \omega_\nu, \text{heuristic} = \text{Haversine})$
- 4: $X_{\mathcal{P}_\nu}^\nu = 1$ if $\sum_{e \in \mathcal{P}} d(e) < \infty$ else 0
- 5: **end for**
- 6: **return** $\{X_{\mathcal{P}_\nu}^\nu\}_\nu$

has already been used in the context of ToD [6] and fits well in network graphs composed by a large amount of nodes [11]. This is mainly because the search is guided by a heuristic function (the Haversine distance is the most commonly used function). To further reduce the time taken by the algorithm to calculate the shortest path in our scenario, all the roads not meeting the service requirements are pruned from the network graph (line 1 in Algorithm 1).

By using the A^* algorithm, the shortest path for each vehicle ν from a source s_ν to a destination d_ν is determined (line 3). We have modified the A^* algorithm so that it satisfies constraint (12). The idea is that by using a weight function ω_ν , defined in Eq.(15), the A^* algorithm will not steer vehicles through routes that contain road sections that cannot admit more vehicles. Instead, the A^* algorithm will choose paths having the radio resources needed to support the vehicle's communications while meeting the latency requirement of the service (D ms) with a reliability level of 99.999%.

The weigh function defined in Eq.(15) assigns a road section a cost of infinity if its capacity ($\nu_e^{\max}(D, \mu, b, L)$) is exhausted

$$\omega_\nu(e) = \begin{cases} \tau(e), & V_\nu(e) < \nu_e^{\max}(D, \mu, b, L) \\ \infty, & V_\nu(e) \geq \nu_e^{\max}(D, \mu, b, L) \end{cases} \quad (15)$$

with $V_\nu(e)$ denoting the number of vehicles that traverse road section e at the same time as vehicle ν :

$$V_\nu(e) = |\nu' \neq \nu : [\tau_{\nu'}(e^+), \tau_{\nu'}(e^-)] \cap [\tau_\nu(e^+), \tau_\nu(e^-)] \neq \emptyset| \quad (16)$$

In conclusion, the algorithm will deny the remote operation of a vehicle if all the possible paths between the source and the destination include a road section without capacity. Otherwise, the vehicle that is requesting the route is admitted, as line 4 in Algorithm 1 shows. It is worth remarking that, contrary to [6], TOVAC considers the time dimension and does not pitfall into static routing.

IV. PERFORMANCE EVALUATION

For validation and insight into the behavior of our proposed admission control and routing algorithm, we have implemented TOVAC in Python using the NetworkX [12] package to build Section II-C capacity graph G . Each road segment $e \in G$ corresponds to an OpenStreetMap [13] nodeway of Turin (Italy) city center. Additionally, we resort to the tractable channel model considered in [7], [8], and use the SINR CCDF expression obtained in Corollary 1 to know the 99.999 SINR.

TABLE I
 EXPERIMENTAL NR SETUP

Parameter	Value	Parameter	Value
Service bitrate b	25 Mbps [2]	Pkt. len. L	12 kb
PDB	5 ms	Numerology μ	2 [7]
NRB _r (T_S^μ , 80 MHz)	108 RB [15]	Freq.	FR2 26 GHz [16]
OH	0.14 [17]	Bandw. B	[80, 320] MHz [16]
Pathloss exp. α	4 [18]	Decode ϵ_r	10^{-5} [19]

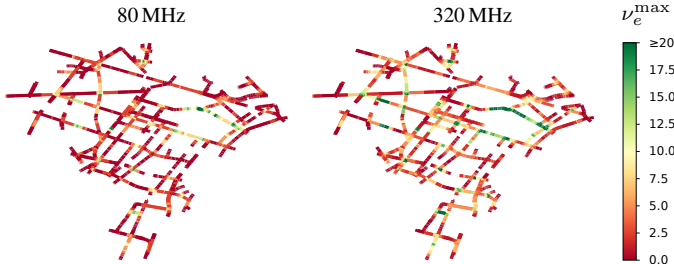


Fig. 2. Heatmaps with the maximum number of remote driving vehicles that can be operated with 99.999% reliability in Turin.

For coverage information, we have used the open data provided by OpenCellID¹, a database of cell towers. In particular, we consider that 5G cell coordinates correspond to the location of LTE cell towers of the network operator with MNC 1 in Turin. If multiple road segments $E' \subset E(G)$ are only served by a single LTE cell – i.e. $\exists! r : e \in E(r), \forall e \in E'$ – we consider a 5G deployment with a dedicated cell per road. We capture such consideration by setting $\nu_r(e) = 1, \forall e \in E'$. Note the consideration holds given the necessity of denser deployments in cellular mmWave.

We have applied the NR configuration described in Table I to each cell. In the experiments we consider four possible channel bandwidths in the Frequency Range (FR) 2, namely: $B = [80, 160, 240, 320]$ MHz. Note that, in Italy, the allocation to individual operators in the 26 GHz band is 200 MHz [14], which means that several of the considered bandwidths are optimistic.

We conduct a comprehensive set of experiments defined as follows. Each experiment ε consists of $V_\varepsilon = 5v + 1, v = 0, \dots, 20$ concurrent vehicle requests, with $S_\varepsilon = |\{s_i\}_{i=1}^{V_\varepsilon}| = \lceil V_\varepsilon/2^s \rceil, s \geq 0$ sources; and $D_\varepsilon = |\{d_i\}_{i=1}^{V_\varepsilon}| = \lceil V_\varepsilon/2^d \rceil, d \geq 0$ destinations. Each vehicle ν_i is randomly assigned to a source $s_{\nu_i} \in \{s_i\}_{i=1}^{V_\varepsilon}$ and a destination $d_{\nu_i} \in \{d_i\}_{i=1}^{V_\varepsilon}$. Each experiment ε restricts/allows all vehicles to (i) share same source and destination, i.e. $2^d, 2^s > V_\varepsilon$; (ii) have completely different destinations $d = s = 0$; or (iii) have a mix of shared/different destinations $0 < d, s < V_\varepsilon$.

Only the uplink traffic, the most demanding, is analyzed, with each vehicle sending 25 Mbps video stream traffic ($L = 12$ kb) with a PDB of 5 ms. The speed of the vehicles is, in each traversed road $e \in G$, equal to the maximum speed of that road e .

Fig. 2 shows two heatmaps of the area of Turin where we have evaluated TOVAC. Each heatmap represents the number

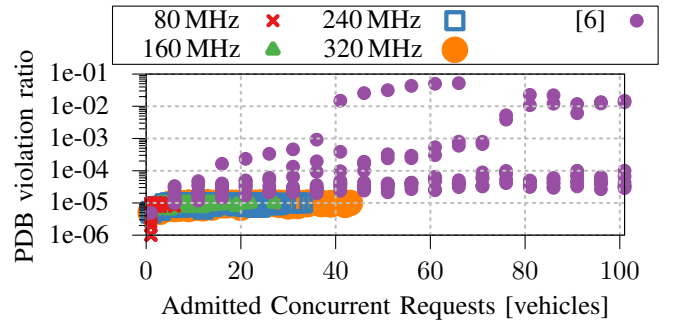


Fig. 3. PDB violation ratio (y-axis) experienced among the admitted vehicles (x-axis).

of vehicles that can be remotely driven on each road segment with 99.999% reliability – i.e., each heatmap represents the capacity graph G . Greener colors mean that more vehicles can be served in the corresponding road segment (the greenest color is dedicated to segments that allow $\nu_e^{\max} = 20$ or more vehicles, with some cases reaching more than $\nu_e^{\max} = 30$). In one heatmap, the available uplink bandwidth for the remote driving service is $B = 80$ MHz, and in the other it is $B = 320$ MHz (the extreme cases). The figure shows the challenges of providing the reliability and data rate required by the ToD service if cells are co-located with LTE cell towers.

An important feature of TOVAC is its ability to keep PDB violations below the 99.999% threshold. This is illustrated in Fig. 3. This figure shows, for the different bandwidths B , the concurrent requests (ToD vehicles) admitted for each realization of the different experiments (defined by the number of vehicles requesting the ToD service), and the resulting PDB violations. Using TOVAC, the fraction of packets sent that result in PDB violations is always kept below 10^{-5} . This is calculated by measuring the number of vehicles coinciding on the same road segment at the same time range, and the SE given the worst case SINR and the resulting MCS on the road segment. With TOVAC, it never happens that more vehicles coincide on a road segment than those that guarantee the PDB, and PDB violations are the result of situations in which the SINR does not achieve the expected values, thus, resulting in packet delays $D > 5$ ms. We also compare our approach with the solution in [6], where, as shown in Fig. 3, there are more vehicles admitted for tele-operation, in fact, all vehicle requests are admitted. However, the PDB violations are greater than 10^{-5} and can reach values close to 10^{-1} – i.e., one out of ten ToD packets violate the PDB. Note that in our implementation of [6], we do not reduce the speed of the vehicles. Nevertheless, reducing the speed as required by [6] would mean that the vehicles would be on the roads longer and more PDB violations would occur.

We also explored the effect of relaxing the 99.999% reliability requirement. In Fig. 4, for the $B = 240$ MHz bandwidth scenario, we compare the admitted vehicles for 99.999%, 99.99%, and 99.9% reliability requirements. As it can be seen in the figure, the number of admitted vehicles for the different realizations of the experiments is significantly increased, both for 99.99% and for 99.9% reliability thresholds, in many cases

¹OpenCellID, largest Open Database of Cell Towers & Geolocation - by Unwired Labs, <https://opencellid.org/>.

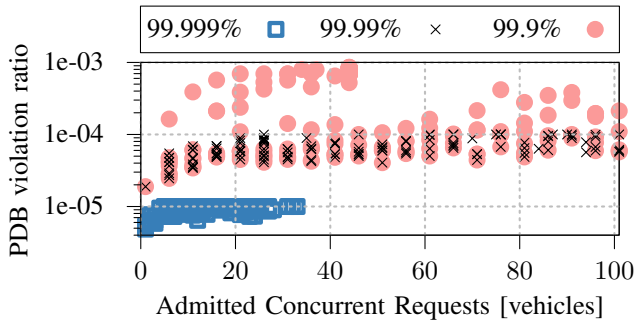


Fig. 4. PDB violation ratio (y-axis) experienced among the admitted vehicles (x-axis) for different reliability requirements, with 240MHz bandwidth.

admitting 100 % of the requests (compare Fig. 4 with the case of the implementation of [6] in Fig. 3). The downside is that the number of PDB violations also increases, although it is still smaller than the number of PDB violations in [6].

Finally, it is interesting to highlight that even if the bandwidth required by the ToD service appears to be very high, the actual use of the radio resources is much smaller. For example, the average consumption of radio resources was of a 10.19% in a stretch of Via Vittorio Emanuele II – a main road in Turin experiencing the highest resource usage. Such result was observed during the realization of experiment ε with $V_\varepsilon = 101$ vehicles traveling from different sources and destinations ($s = d = 0$) and $B = 240$ MHz of available uplink bandwidth. By employing an elastic slice [20] to implement the reservation of resources for the ToD service, the unused resources could be exploited by other users while the vehicles are not using them, so providing the ToD service can be much less onerous for the operator than it might appear.

V. CONCLUSION

ToD services require reliable, high-bandwidth, and low-latency communications to ensure that the same safety level or better than traditional driving is achieved. In this letter, the TOVAC algorithm has been proposed to prevent vehicular traffic from exhausting the available 5G network resources. TOVAC estimates the 99.999 SINR percentile that tele-operated vehicles experiment at each road to perform admission control and routing decisions that meet the ToD QoS. The obtained results show that all the vehicles admitted by TOVAC obtain a service that meets the bandwidth, latency and reliability requirements defined in the 3GPP standards. Although it may seem that the number of vehicles admitted is very limited (around 50 in the best scenario), results show that TOVAC keeps a rather small network utilisation (up to about 10,19% on average for the busiest road section). This opens the door to keep pursuing the work on new and efficient online route planning algorithms, for example, to adapt the routes to the actual network conditions that vehicles are measuring along the route.

REFERENCES

- [1] O. Amador, M. Aramrattana, and A. Vinel, "A Survey on Remote Operation of Road Vehicles," *IEEE Access*, vol. 10, pp. 130 135–130 154, Dec. 2022.
- [2] *Enhancement of 3GPP support for V2X scenarios*, 3GPP TS 22.186 V17.0.0, 2022.
- [3] Kousaridas *et al.*, "QoS Prediction for 5G Connected and Automated Driving," *IEEE Commun. Mag.*, vol. 59, no. 9, pp. 58–64, 2021.
- [4] "Making 5G Proactive and Predictive for the Automotive Industry," 5GAA, München, Germany, 2019. [Online]. Available: https://5gaa.org/content/uploads/2020/01/5GAA_White-Paper_Proactive-and-Predictive_v04_8-Jan.-2020-003.pdf
- [5] *System architecture for the 5G System (5GS)*, 3GPP TS 23.501 V18.1.0, 2023.
- [6] G. Liu, S. Salehi, E. Bala, C.-C. Shen, and L. J. Cimini, "Communication-Constrained Routing and Traffic Control: A Framework for Infrastructure-Assisted Autonomous Vehicles," *IEEE Trans. on Intell. Transp. Syst.*, vol. 23, no. 12, pp. 23 844–23 857, 2022.
- [7] O. Adamuz-Hinojosa, V. Sciancalepore, P. Ameigeiras, J. M. Lopez-Soler, and X. Costa-Pérez, "A Stochastic Network Calculus (SNC)-Based Model for Planning B5G uRLLC RAN Slices," *IEEE Trans. on Wireless Commun.*, vol. 22, no. 2, pp. 1250–1265, 2023.
- [8] J. G. Andrews, F. Baccelli, and R. K. Ganti, "A Tractable Approach to Coverage and Rate in Cellular Networks," *IEEE Trans. on Commun.*, vol. 59, no. 11, pp. 3122–3134, 2011.
- [9] *NR; Physical layer procedures for data*, 3GPP TS 38.214 V17.6.0, 2023.
- [10] A. Hall, S. Hippler, and M. Skutella, "Multicommodity flows over time: Efficient algorithms and complexity," *Theoretical Computer Science*, vol. 379, no. 3, pp. 387–404, 2007.
- [11] Duan *et al.*, "Finding the shortest path in huge data traffic networks: A hybrid speed model," in *2015 IEEE Int. Conf. on Commun. (ICC)*, London, UK, 2015, pp. 6906–6911.
- [12] A. A. Hagberg, D. A. Schult, and P. J. Swart, "Exploring network structure, dynamics, and function using NetworkX," in *Proc. of the 7th Python in Science Conf. (SciPy2008)*, Pasadena, CA USA, 2008, pp. 11–15.
- [13] OpenStreetMap contributors, "Planet dump retrieved from <https://planet.osm.org>," <https://www.openstreetmap.org>, 2017.
- [14] Autorità per le Garanzie nelle Comunicazioni, "Procedura per l'assegnazione e regole per l'utilizzo delle frequenze disponibili nelle bande 694-790 MHz, 3600-3800 MHz e 26.5-27.5 GHz per sistemi terrestri di comunicazioni elettroniche al fine di favorire la transizione verso la tecnologia 5G, ai sensi della legge 27 dicembre 2017, n. 205," dec 2017.
- [15] *NR; Base Station (BS) radio transmission and reception*, 3GPP TS 38.104 V18.2.0, 2023.
- [16] C. A. Haro, "5G and Beyond Activities Promoted by Member States," 5G Infrastructure Association (5G-IA), 2020. [Online]. Available: https://5g-ppp.eu/wp-content/uploads/2020/12/201209-Member_State_Initiatives_5G_FINAL.pdf
- [17] *NR; User Equipment (UE) radio access capabilities*, 3GPP TS 38.306 V17.5.0, 2023.
- [18] L. Yang, F.-C. Zheng, and S. Jin, "Spatio-Temporal Analysis of SINR Meta Distribution for mmWave Heterogeneous Networks Under Geo/G/1 Queues," in *IEEE 95th Vehicular Technol. Conf. (VTC)*, 2022, pp. 1–6.
- [19] Y. Polyanskiy, H. V. Poor, and S. Verdú, "Channel Coding Rate in the Finite Blocklength Regime," *IEEE Trans. on Inf. Theory*, vol. 56, no. 5, pp. 2307–2359, 2010.
- [20] Okic *et al.*, " π -ROAD: a Learn-as-You-Go Framework for On-Demand Emergency Slices in V2X Scenarios," in *IEEE Conference on Computer Communications (INFOCOM)*, Vancouver, BC, Canada, 2021, pp. 1–10.